

# Synthesis and Properties of Noncoplanar Rigid-Rod Aromatic Polyhydrazides and Poly(1,3,4-oxadiazole)s Containing Phenyl or Naphthyl Substituents

GUEY-SHENG LIOU,<sup>1</sup> SHENG-HUEI HSIAO,<sup>2</sup> YI-KAI FANG<sup>1</sup>

<sup>1</sup>Department of Applied Chemistry, National Chi Nan University, Nantou Hsien 545, Taiwan, Republic of China

<sup>2</sup>Department of Chemical Engineering, Tatung University, Taipei 104, Taiwan, Republic of China

Received 10 July 2006; accepted 19 August 2006

DOI: 10.1002/pola.21747

Published online in Wiley InterScience (www.interscience.wiley.com).

**ABSTRACT:** Two new phenyl- and naphthyl-substituted rigid-rod aromatic dicarboxylic acid monomers, 2,2'-diphenylbiphenyl-4,4'-dicarboxylic acid (**4**) and 2,2'-di(1-naphthyl)biphenyl-4,4'-dicarboxylic acid (**5**), were synthesized by the Suzuki coupling reaction of 2,2'-diiodobiphenyl-4,4'-dicarboxylic acid dimethyl ester with benzenboronic acid and naphthaleneboronic acid, respectively, followed by alkaline hydrolysis of the ester groups. Four new polyhydrazides were prepared from the dicarboxylic acids **4** and **5** with terephthalic dihydrazide (TPH) and isophthalic dihydrazide (IPH), respectively, via the Yamazaki phosphorylation reaction. These polyhydrazides were amorphous and readily soluble in many organic solvents. Differential scanning calorimetry (DSC) indicated that these hydrazide polymers had glass transition temperatures in the range of 187–234 °C and could be thermally cyclodehydrated into the corresponding oxadiazole polymers in the range of 300–400 °C. The resulting poly(1,3,4-oxadiazole)s exhibited  $T_g$ 's in the range of 252–283 °C, 10% weight-loss temperature in excess of 470 °C, and char yield at 800 °C in nitrogen higher than 54%. These organo-soluble polyhydrazides and poly(1,3,4-oxadiazole)s exhibited UV–Vis absorption maximum at 262–296 and 264–342 nm in NMP solution, and their photoluminescence spectra showed maximum bands around 414–445 and 404–453 nm, respectively, with quantum yield up to 38%. The electron-transporting properties were examined by electrochemical methods. Cyclic voltammograms of the poly(1,3,4-oxadiazole) films cast onto an indium-tin oxide (ITO)-coated glass substrate exhibited reversible reduction redox with  $E_{\text{onset}}$  at  $-1.37$  to  $-1.57$  V versus Ag/AgCl in dry *N,N*-dimethylformamide solution. © 2006 Wiley Periodicals, Inc. *J Polym Sci Part A: Polym Chem* 44: 6466–6483, 2006

**Keywords:** electrochemistry; luminescence; polyhydrazides; polyoxadiazoles; 2,2'-disubstituted 4,4'-biphenyldicarboxylic acids

## INTRODUCTION

Heterocyclic aromatic poly(1,3,4-oxadiazole)s have been extensively studied for a long time due to their high thermal and chemical stabil-

ity.<sup>1,2</sup> Recently, the use of conjugated polymers as polymer light-emitting diodes (LEDs) has received a great deal of concern in academia and the optoelectronic industry because of their several appealing advantages over other technologies.<sup>3</sup> Electron affinity was improved when the electron-withdrawing moieties of aryl-substituted 1,3,4-oxadiazole were incorporated into conjugated polymer main chain or attached as

Correspondence to: G.-S. Liou (E-mail: gsliau@ncnu.edu.tw)

*Journal of Polymer Science: Part A: Polymer Chemistry*, Vol. 44, 6466–6483 (2006)  
© 2006 Wiley Periodicals, Inc.

side groups.<sup>4–9</sup> Thus, 1,3,4-oxadiazole-containing conjugated polymers have been widely investigated and applied as electron transport or emission layers in LEDs.<sup>10–13</sup> Unfortunately, most of the light-emitting polymers with electron-withdrawing 1,3,4-oxadiazole units in side or main chains exhibit poor solubility and infusibility that limits their application. Many efforts have been made to improve the solubility and lower  $T_g$  and hence to make such polymers to be processed more easily, for example by incorporating flexible linkages in the backbone or bulky pendant group on the aromatic ring.<sup>14–20</sup>

Oxadiazoles, such as 2-(4-biphenyl)-5-(4-*tert*-butylphenyl)-1,3,4-oxadiazole (PBD), have long been some of the most favorable compounds in organic light-emitting diodes (OLEDs) as electron-conducting/hole-blocking materials. However, the efficiency was limited due to their crystallization during the operation of LED. This problem was mitigated by incorporation of the electron-transporting units into the main chain or side chain attached to the backbone of a polymer.<sup>21–23</sup> Several different reaction pathways have been developed to prepare poly(1,3,4-oxadiazole)s.<sup>24–28</sup> The most popular process involves the preparation of a precursor polyhydrazide by the reaction of dicarboxylic acids or diacid chlorides with hydrazine hydrate or dihydrazides, followed by cyclodehydration of the intermediate polyhydrazides.<sup>29–31</sup>

This article reports the synthesis and characterization of some novel noncoplanar rigid-rod aromatic polyhydrazides and the corresponding poly(1,3,4-oxadiazole)s by the use of 2,2'-disubstituted 4,4'-biphenyldicarboxylic acids (substituents are phenyl and 1-naphthyl). In general, introduction of bulky group into 2,2'-position of biphenyl moiety will produce higher levels of ring-torsion, and thus induce noncoplanar structure. The noncoplanar biphenyl units would disrupt close chain packing and provide enhanced solubility. Besides solubility and thermal properties, the photoluminescent and electrochemical properties of the newly synthesized polymers are reported herein.

## EXPERIMENTAL

### Materials

Reagent-grade 4,4'-biphenyldicarboxylic acid dimethyl ester (Tokyo Chemical Industries),  $\text{Ag}_2\text{SO}_4$  (SHOWA),  $\text{I}_2$  (Lancaster),  $\text{Na}_2\text{CO}_3$  (SHOWA),  $\text{Pd}(\text{PPh}_3)_4$  (Lancaster), 1-naphthaleneboronic acid

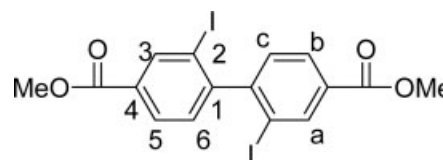
(Lancaster), benzenboronic acid (Lancaster),  $\text{H}_2\text{SO}_4$  (SHOWA), toluene (TEDIA), *N*-methyl-2-pyrrolidinone (NMP) (TEDIA), *N,N*-dimethylacetamide (DMAc) (TEDIA), pyridine (Py) (TEDIA), and diphenyl phosphite (DPP) (ACROS) were used as received. Terephthalic dihydrazide (TPH) and isophthalic dihydrazide (IPH) were purchased from TCI and used without further purification. Commercially obtained anhydrous calcium chloride ( $\text{CaCl}_2$ ) was dried under vacuum at 180 °C for 8 h. Tetrabutylammonium perchlorate (TBAP) (ACROS) was recrystallized twice from ethyl acetate and then dried *in vacuo* prior to use. All other reagents were used without further purification.

### Monomer Synthesis

#### 2,2'-Diiodobiphenyl-4,4'-dicarboxylic acid dimethyl ester (1)<sup>32</sup>

Into a solution of 10.22 g (37.8 mmol) of 4,4'-biphenyldicarboxylic acid dimethyl ester and 34.61 g (111.0 mmol) of silver sulfate in 110 mL of  $\text{H}_2\text{SO}_4$  (97%), 25.58 g (100.8 mmol) of iodine was added. The mixture was heated with stirring at 80 °C for 36 h under nitrogen and then the purple reaction mixture was poured into 2.5 L of  $\text{Na}_2\text{SO}_3(\text{aq})$  at ice bath. The yellow suspension was extracted with ethyl acetate. The organic layer was collected, dried over anhydrous  $\text{MgSO}_4$ , and concentrated under vacuum to give a corn-colored solid (17.64 g, 94%), which was esterified in refluxing 75 mL of methanol for 24 h, using 2 mL of  $\text{H}_2\text{SO}_4$  as a catalyst. The mixture was extracted with dichloromethane, washed with  $\text{NaHCO}_3(\text{aq})$ , dried over anhydrous  $\text{MgSO}_4$ , and concentrated under reduced pressure to give a white solid (16.63 g, 89%). The purification was by recrystallization from methanol to give white crystals (14.39, 77%); mp 154–157 °C [lit.<sup>21</sup> 152–153 °C] measured by DSC at 10 °C/min.

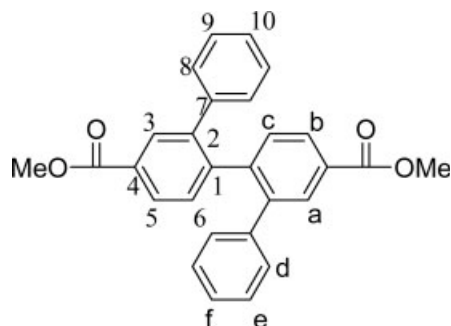
IR (KBr): 2948  $\text{cm}^{-1}$  (C–H), 1712  $\text{cm}^{-1}$  (C=O).  $^1\text{H}$ -NMR (400 MHz,  $\text{CDCl}_3$ ,  $\delta$ , ppm): 8.61 (s, 2H,  $\text{H}_a$ ), 8.09 (d,  $J = 8.0$  Hz, 2H,  $\text{H}_b$ ), 7.24 (d,  $J = 8.0$  Hz, 2H,  $\text{H}_c$ ), 3.95 (s, 6H,  $-\text{CH}_3$ ).  $^{13}\text{C}$ -NMR (100 MHz,  $\text{CDCl}_3$ ,  $\delta$ , ppm): 165.18 (C=O), 152.29 ( $\text{C}^1$ ), 140.11 ( $\text{C}^4$ ), 131.33 ( $\text{C}^3$ ), 129.42 ( $\text{C}^6$ ), 129.27 ( $\text{C}^5$ ), 98.32 ( $\text{C}^2$ ), 53.49 ( $-\text{CH}_3$ ).



**2,2'-Diphenylbiphenyl-4,4'-dicarboxylic acid dimethyl ester (2)**<sup>32</sup>

A solution of 5.48 g (10.5 mmol) of compound **1**, 4.36 g (35.7 mmol) of 1-benzeneboronic acid, 0.58 g (0.5 mmol) of Pd(PPh<sub>3</sub>)<sub>4</sub>, and 5.35 g (50.0 mmol) of Na<sub>2</sub>CO<sub>3</sub> in 24 mL of toluene, 4.8 mL of ethanol, and 33 mL of H<sub>2</sub>O was heated at 80 °C under nitrogen atmosphere for 14 h. The crude product was extracted with ethyl acetate several times. The organic layer was collected, dried over anhydrous MgSO<sub>4</sub> and concentrated under vacuum to give an ash gray solid (3.64 g, 81%). Further purification of the crude product by recrystallization from methanol/toluene gave pale gray crystals (2.73 g, 61%); mp 215–218 °C measured by DSC at 10 °C/min.

IR (KBr): 2952 cm<sup>-1</sup> (C—H), 1718 cm<sup>-1</sup> (C=O), 1108, 1242 cm<sup>-1</sup> (C—O). <sup>1</sup>H-NMR (400 MHz, CDCl<sub>3</sub>, δ, ppm): 8.04 (dd, *J* = 8.0, 1.6 Hz, 2H, H<sub>b</sub>), 7.87 (d, *J* = 1.6 Hz, 2H, H<sub>a</sub>), 7.48 (d, *J* = 8.0 Hz, 2H, H<sub>c</sub>), 7.11 (t, *J* = 7.6 Hz, 2H, H<sub>f</sub>), 7.01 (t, *J* = 7.6 Hz, 4H, H<sub>e</sub>), 6.61 (d, *J* = 7.6 Hz, 4H, H<sub>d</sub>). <sup>13</sup>C-NMR (100 MHz, CDCl<sub>3</sub>, δ, ppm): 166.79 (C—O), 143.77 (C<sup>1</sup>), 141.18 (C<sup>7</sup>), 139.50 (C<sup>2</sup>), 131.55 (C<sup>6</sup>), 131.31 (C<sup>3</sup>), 129.70 (C<sup>4</sup>), 129.08 (C<sup>8</sup>), 128.12 (C<sup>5</sup>), 127.70 (C<sup>9</sup>), 126.69 (C<sup>10</sup>), 52.14 (CH<sub>3</sub>).

**2,2'-Di(1-naphthyl)biphenyl-4,4'-dicarboxylic acid dimethyl ester (3)**<sup>33</sup>

Compound **3** was prepared by the similar procedure as compound **2** affording a white solid (4.40 g, 100%) and purified by recrystallization from methanol and CHCl<sub>3</sub> to give white powder (3.52 g, 80%); mp 183–186 °C [lit.<sup>22</sup> 186–187 °C] measured by DSC at 10 °C/min.

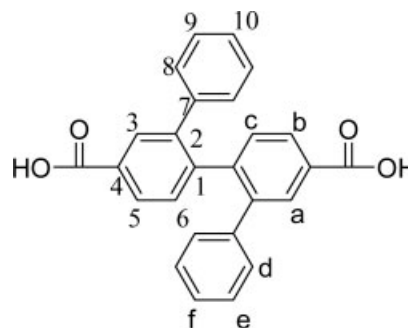
IR (KBr): 2949 cm<sup>-1</sup> (C—H), 1718 cm<sup>-1</sup> (C=O), 1259 and 1113 cm<sup>-1</sup> (C—O). The quality of the <sup>13</sup>C-NMR was relatively good but still showed some coalesced broad signals. Therefore, only the sharp signals were picked up and reported here. <sup>13</sup>C-NMR (100 MHz, CDCl<sub>3</sub>, δ, ppm): 166.77, 166.70, 145.18,

139.05, 137.00, 133.62, 133.03, 132.81, 132.68, 131.97, 128.67, 127.92, 127.86, 127.72, 125.88, 125.69, 125.40, 124.44, and 52.09.

**2,2'-Diphenylbiphenyl-4,4'-dicarboxylic acid (4)**

A mixture of 2.44 g (43.5 mmol) potassium hydroxide and 1.40 g (3.3 mmol) of the obtained dimethyl ester compound **3** in 10 mL of ethanol and 30 mL of distilled water was stirred at ~100 °C for 10 h. The solution was cooled, and the pH value was adjusted by hydrochloric acid to near 3. The crude white solid precipitate was filtered and recrystallized from acetic acid and water to give white powder (1.05 g, 81%); mp 357–360 °C measured by DSC at 10 °C/min.

IR (KBr): 2700–3400 cm<sup>-1</sup> (O—H), 1681 cm<sup>-1</sup> (C=O). <sup>1</sup>H-NMR (500 MHz, DMSO-*d*<sub>6</sub>, δ, ppm): 13.15 (br, 2H, —COOH), 7.97 (dd, *J* = 8.0, 1.9 Hz, 2H, H<sub>b</sub>), 7.71 (d, *J* = 1.9 Hz, 2H, H<sub>a</sub>), 7.54 (d, *J* = 8.0 Hz, 2H, H<sub>c</sub>), 7.19 (t, *J* = 7.4 Hz, 2H, H<sub>f</sub>), 7.10 (t, *J* = 7.7 Hz, 4H, H<sub>e</sub>), 6.62 (d, *J* = 7.4 Hz, 4H, H<sub>d</sub>). <sup>13</sup>C-NMR (125 MHz, DMSO-*d*<sub>6</sub>, δ, ppm): 166.86 (C=O), 142.89 (C<sup>1</sup>), 140.44 (C<sup>7</sup>), 139.14 (C<sup>2</sup>), 131.74 (C<sup>6</sup>), 130.43 (C<sup>3</sup>), 130.38 (C<sup>4</sup>), 128.61 (C<sup>8</sup>), 127.98 (C<sup>5</sup>), 127.73 (C<sup>9</sup>), 126.68 (C<sup>10</sup>). ANAL. CALCD for C<sub>26</sub>H<sub>18</sub>O<sub>4</sub> (394.12): C, 79.17%; H, 4.60%. Found: C, 79.21%; H, 4.57%.

**2,2'-Di(1-naphthyl)biphenyl-4,4'-dicarboxylic acid (5)**

The diacid monomer **5** was prepared by the similar procedure as compound **4** affording a white solid and purified by recrystallization from acetic acid and water to give white powder (0.65 g, 84%); mp 356–359 °C measured by DSC at 10 °C/min.

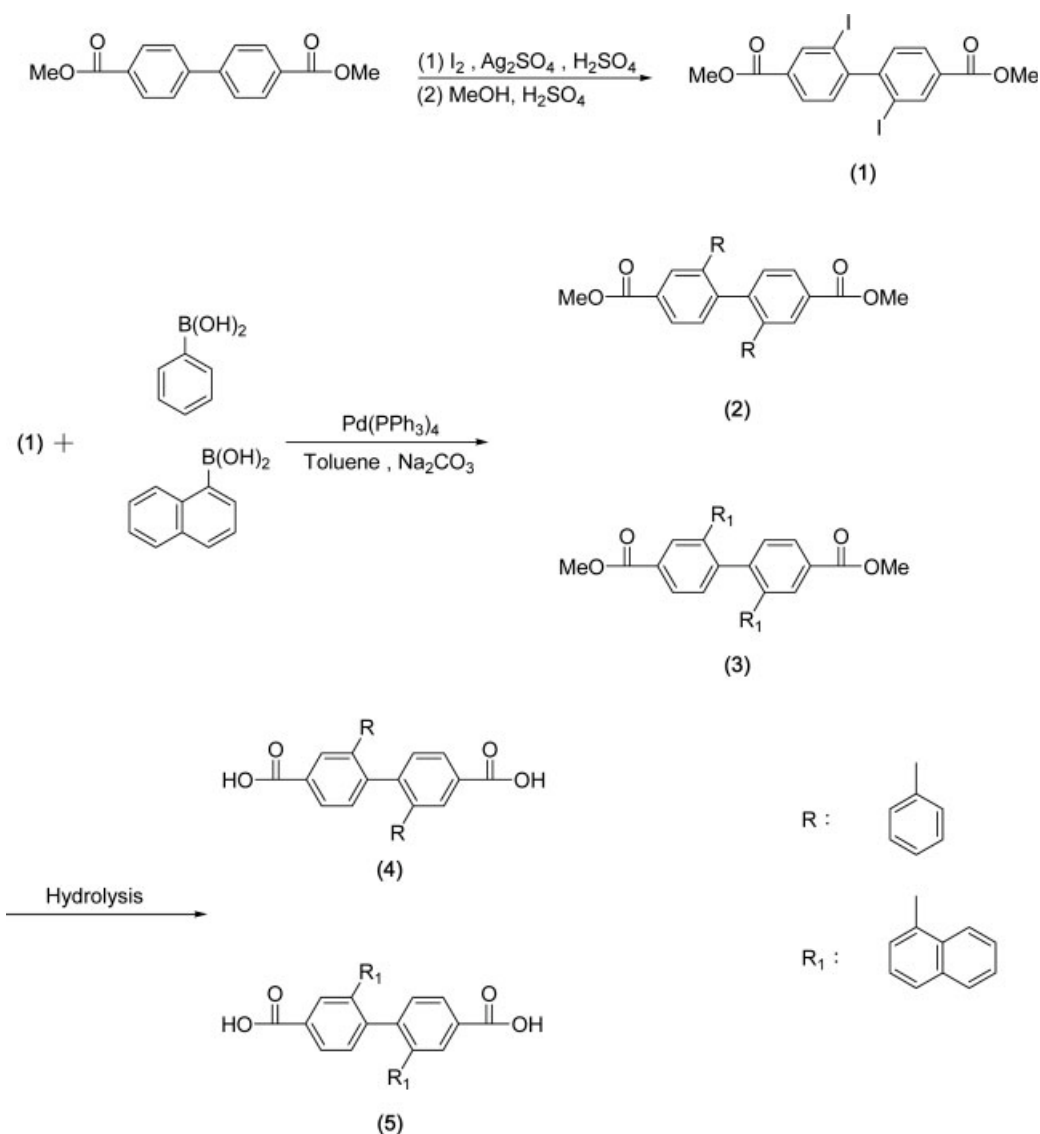
IR (KBr): 2700–3400 cm<sup>-1</sup> (O—H), 1681 cm<sup>-1</sup> (C=O). <sup>1</sup>H-NMR (500 MHz, DMSO-*d*<sub>6</sub>, δ, ppm): 13.15 (s, 2H, —COOH), 5.80–8.13 (Coalesced ArH, 20H). Note that restricted rotation around C—C bonds of the naphthyl–biphenyl groups lead to

coalesced aromatic signals. The quality of the  $^{13}\text{C}$ -NMR is relatively good, but still we can observe some coalesced broad signals. Therefore, only the sharp signals are picked up and reported here.  $^{13}\text{C}$ -NMR (125 MHz,  $\text{DMSO-}d_6$ ,  $\delta$ , ppm): 166.87, 166.73, 144.38, 138.20, 133.19, 132.82, 132.08, 131.86, 130.61, 129.29, 128.37, 127.99, 127.66, 127.43, 125.89, 125.56, 125.22, 124.83, 124.36, 123.79, 123.19. ANAL. CALCD for  $\text{C}_{34}\text{H}_{22}\text{O}_4$  (494.54): C, 82.58%; H, 4.48%. Found: C, 82.62%; H, 4.39%.

### Preparation of Polyhydrazides

The phosphorylation polycondensation method<sup>34</sup> was used to prepare the polyhydrazides pre-

sented in this study. A typical synthetic procedure for polyhydrazide **I-IPH** is described as follows. A dried 50-mL flask was charged with dicarboxylic acid **4** (0.394 g, 1.0 mmol), IPH (0.194 g, 1.0 mmol), NMP (2.0 mL),  $\text{CaCl}_2$  (0.24 g), diphenyl phosphite (DPP) (0.8 mL), and pyridine (0.48 mL). The mixture was heated with stirring at 120 °C for 5 h, and as the polycondensation proceeded the solution became viscous gradually. The resulting highly viscous polymer solution was poured slowly into 200 mL of methanol with stirring, giving a fibrous precipitate that was collected by filtration, washed thoroughly with hot water and methanol. Precipitations from DMAc into methanol were carried out twice for



**Scheme 1.** Synthesis of monomers.

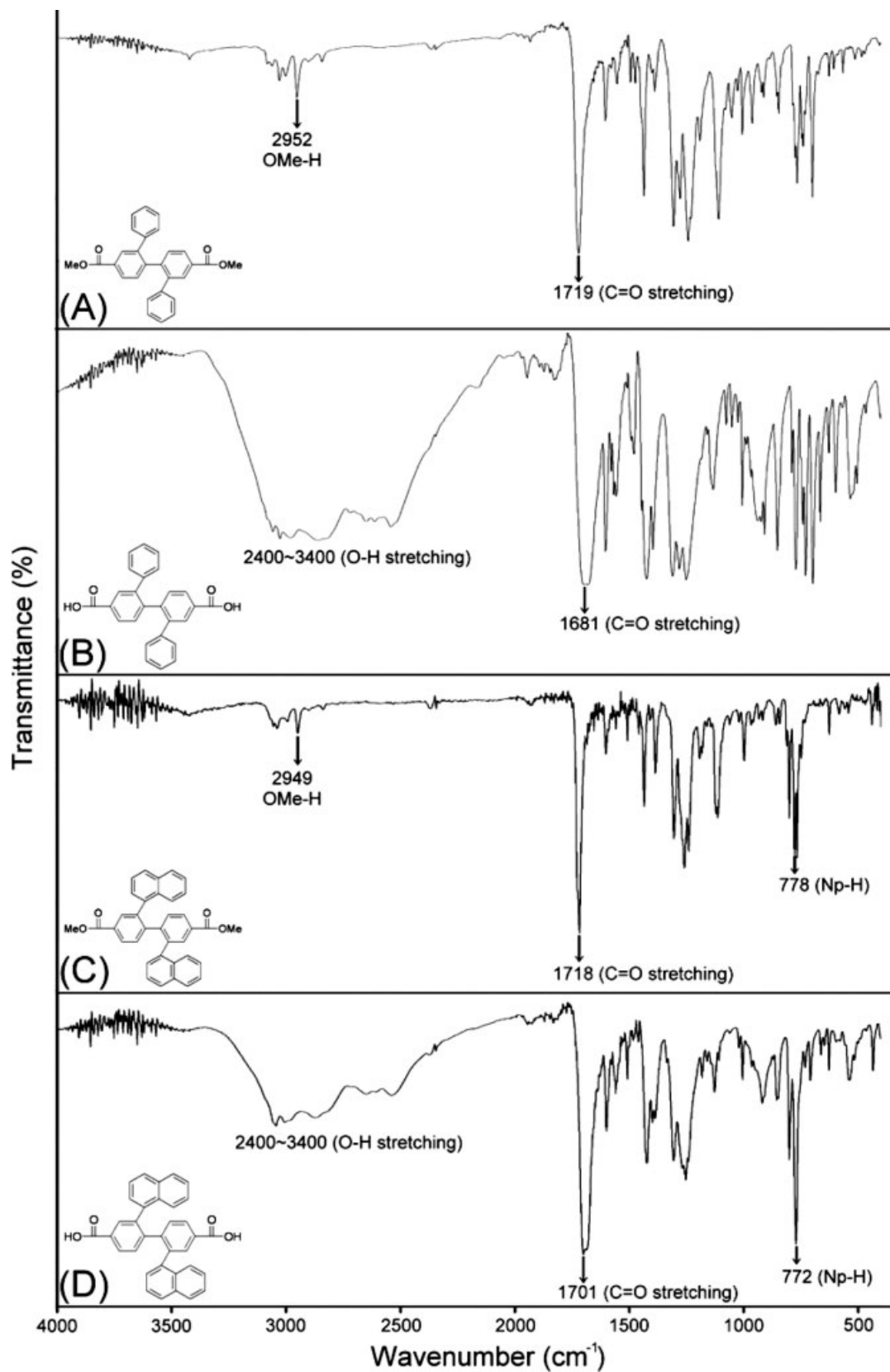


**Figure 1.** IR spectra of (A) dimethyl ester compound **2**, (B) diacid monomer **4**, (C) dimethyl ester compound **3**, and (D) diacid monomer **5**.



further purification. The yield was quantitative, and the inherent viscosity of the polyhydrazide **I-IPH** was 0.36 dL/g as measured in NMP at a concentration of 0.5 g/dL at 30 °C.

IR (film): 3244 (N—H), 1660  $\text{cm}^{-1}$  (C = O).

### Film Preparation and Cyclodehydration of the Hydrazide Polymers

A polymer solution was made by the dissolution of about 0.30 g of the polyhydrazide sample in 4 mL of DMAc. The homogeneous solution was poured into a 4-cm glass Petri dish, which was placed in a 90 °C oven overnight to slowly release the solvent, and then the film was stripped off from the glass substrate and further dried *in vacuo* at 160 °C for 6 h. The obtained films were used as X-ray diffrac-

tion, solubility tests, thermal analyses, optical, and electrochemical properties measurements. The cyclodehydration of the polyhydrazides to the corresponding poly(1,3,4-oxadiazole)s was carried out by heating the above fabricated polymer films at 200 °C for 30 min, 250 °C, 300 °C, and 350 °C for 1 h, respectively, under vacuum.

### Measurements

Infrared spectra were recorded on a PerkinElmer RXI FT-IR spectrometer.  $^1\text{H}$  and  $^{13}\text{C}$ -NMR spectra were measured on a Bruker Avance 500 MHz FT-NMR system. Elemental analyses were run in an Elementar VarioEL-III. The inherent viscosities were determined at 0.5 g/dL concentration using a Tamson TV-2000 viscometer at 30 °C.

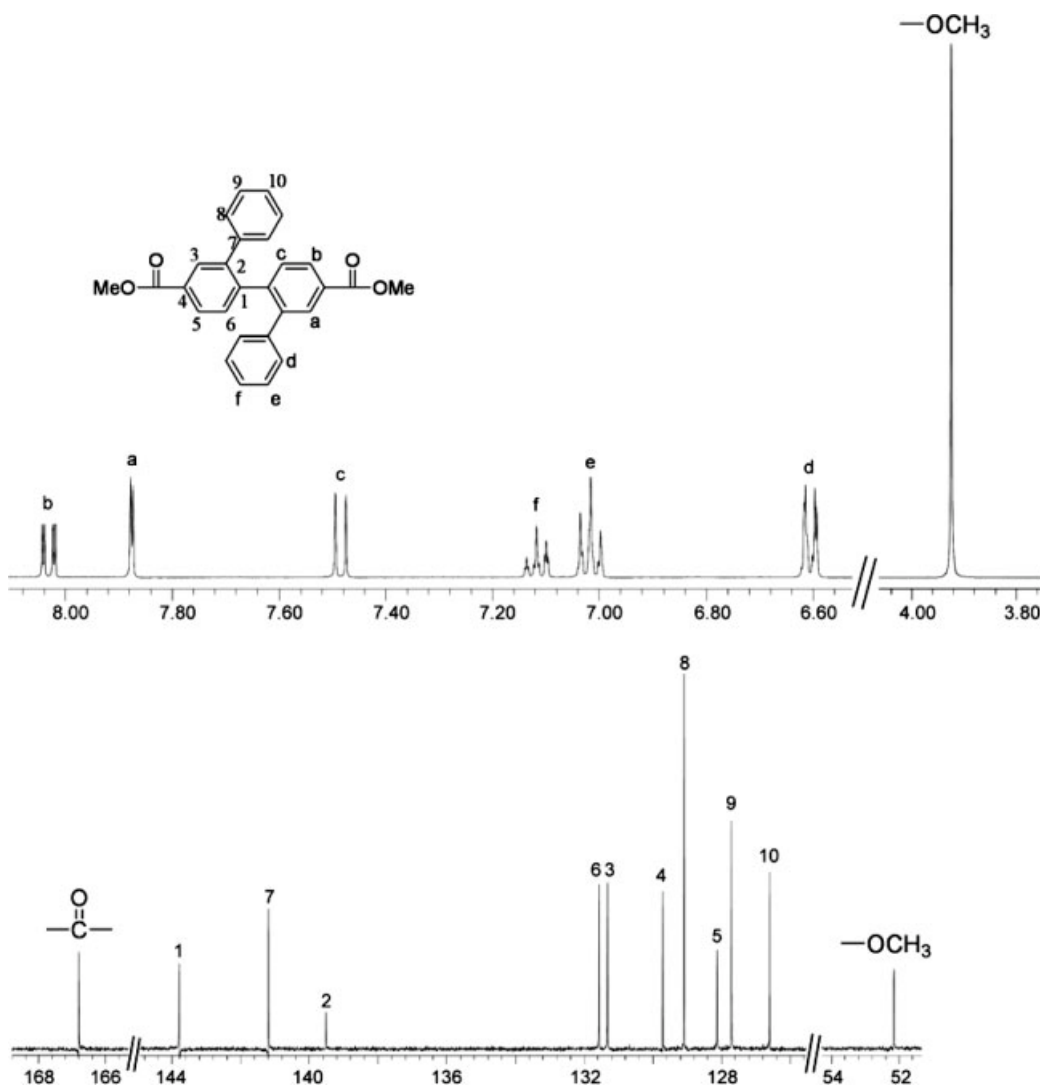


**Figure 2.**  $^1\text{H}$ -NMR and  $^{13}\text{C}$ -NMR spectra of compound **2** in  $\text{CDCl}_3$ .

Wide-angle X-ray diffraction (WAXD) measurements of the polymer films were performed at room temperature ( $\sim 25\text{ }^{\circ}\text{C}$ ) on a Shimadzu XRD-7000 X-ray diffractometer (40 kV, 20 mA) with a graphite monochromator, using nickel-filtered Cu-K $\alpha$  radiation. Ultraviolet-visible (UV-Vis) spectra of the polymer films were recorded on a Varian Cary 50 Probe spectrometer. Thermogravimetric analysis (TGA) was conducted with a PerkinElmer Pyris 1 TGA. Experiments were carried out on  $\sim 6\text{--}8$  mg film samples heated in flowing nitrogen or air (flow rate =  $40\text{ cm}^3/\text{min}$ ) at a heating rate of  $20\text{ }^{\circ}\text{C}/\text{min}$ . DSC analyses were performed on a PerkinElmer Pyris 1 DSC at a scan rate of  $20\text{ }^{\circ}\text{C}/\text{min}$  in flowing nitrogen ( $20\text{ cm}^3/\text{min}$ ). Electrochemistry was performed with a CHI 611B electrochemical analyzer. Voltammograms are presented with the positive potential pointing to the left and with increasing anodic currents pointing downwards. Cyclic voltammetry was performed with the use of a three-electrode cell in which ITO (polymer films area about  $0.7 \times 0.5\text{ cm}^2$ ) was used as a working electrode. A platinum wire was used as an auxiliary electrode. All cell potentials were taken with the use of a homemade Ag/AgCl, KCl (sat.) reference electrode. The spectroelectrochemical cell was composed of a 1-cm cuvette, ITO as a working electrode, a platinum wire as an auxiliary electrode, and a Ag/AgCl reference electrode. Absorption

spectra were measured with a HP 8453 UV-Vis spectrophotometer. Photoluminescence spectra were measured with a Jasco FP-6300 spectrofluorometer. Fluorescence quantum yield ( $\Phi_F$ ) of the samples in NMP were measured by using quinine sulfate in 1 N H $_2$ SO $_4$  as a reference standard ( $\Phi_F = 0.546$ )<sup>35</sup> were used. All corrected fluorescence excitation spectra were found to be equivalent to their respective absorption spectra.

## RESULTS AND DISCUSSION

### Monomer Synthesis

The new phenyl- and naphthyl-substituted non-coplanar rigid-rod aromatic dicarboxylic acid monomers, 2,2'-diphenylbiphenyl-4,4'-dicarboxylic acid (**4**) and 2,2'-di(1-naphthyl)biphenyl-4,4'-dicarboxylic acid (**5**) were synthesized by the Suzuki-reaction from 2,2'-diiodobiphenyl-4,4'-dicarboxylic acid dimethyl ester with benzeneboronic acid and 1-naphthaleneboronic acid, respectively, followed by the subsequent alkaline hydrolysis of the dimethyl ester intermediates as shown in Scheme 1. Elemental analysis, IR, and  $^1\text{H}$  and  $^{13}\text{C}$ -NMR spectroscopic techniques were used to identify the structures of the intermediate dimethyl ester compounds **2** and **3** and the dicarboxylic acid monomers **4** and **5**. Figure 1

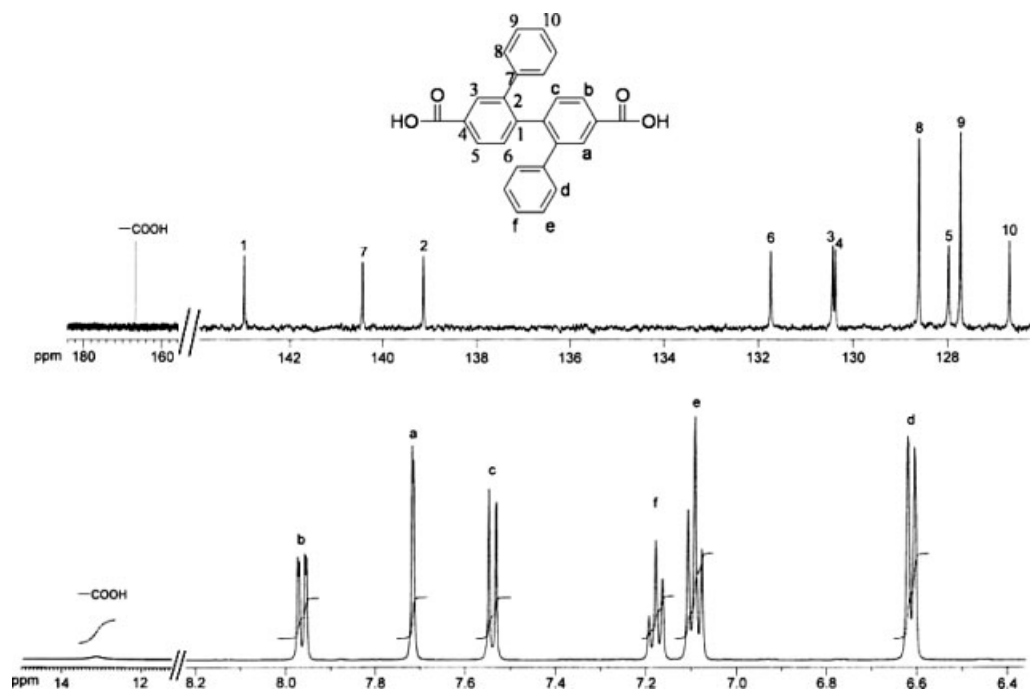


**Figure 3.**  $^1\text{H}$ -NMR and  $^{13}\text{C}$ -NMR spectra of compound **4** in DMSO- $d_6$ .

shows the FTIR spectra of all the synthesized compounds. The ester groups of compounds **2** and **3** give characteristic bands at 1718 and 1719  $\text{cm}^{-1}$  (C—O stretching), respectively. After hydrolysis, the characteristic absorptions of the diacid showed the typical C=O and O—H stretching absorptions at 1700  $\text{cm}^{-1}$  and 2400–3400  $\text{cm}^{-1}$ . Figures 2 and 3 illustrate the  $^1\text{H}$ -NMR and  $^{13}\text{C}$ -NMR spectra of intermediate dimethyl ester compound **2** and dicarboxylic acid monomer **4**. Assignments of each carbon and proton are assisted by the two-dimensional NMR spectra shown in Figures 4 and 5, and these spectra agree well with the proposed molecular structure of monomer **4**.

### Polymer Synthesis

A two-step procedure was employed to obtain the poly(1,3,4-oxadiazole)s from the diacids **4**

and **5** with TPH and IPH (Scheme 2). The first stage consists of the synthesis of hydrazide prepolymers that are converted to the corresponding oxadiazole polymers in the second stage by the thermal cyclodehydration procedure. The polymerization proceeded homogeneously throughout the reaction and afforded clear, highly viscous polymer solutions. All the hydrazide prepolymers precipitated in a tough fiber-like form when slowly pouring the resulting polymer solutions into methanol. The obtained polyhydrazides had inherent viscosities in the range of 0.34–0.97 dL/g as shown in Table 1. Thermal conversion of the hydrazide group to the 1,3,4-oxadiazole ring could be monitored with FTIR. As a representative study, a thin-film sample of polyhydrazide **II-TPH** was heated for 1 h at 350 °C. The IR spectra of this sample are shown in Figure 6. After curing at 350 °C for 1 h, polyhydrazide **II-TPH** was completely cyclized into

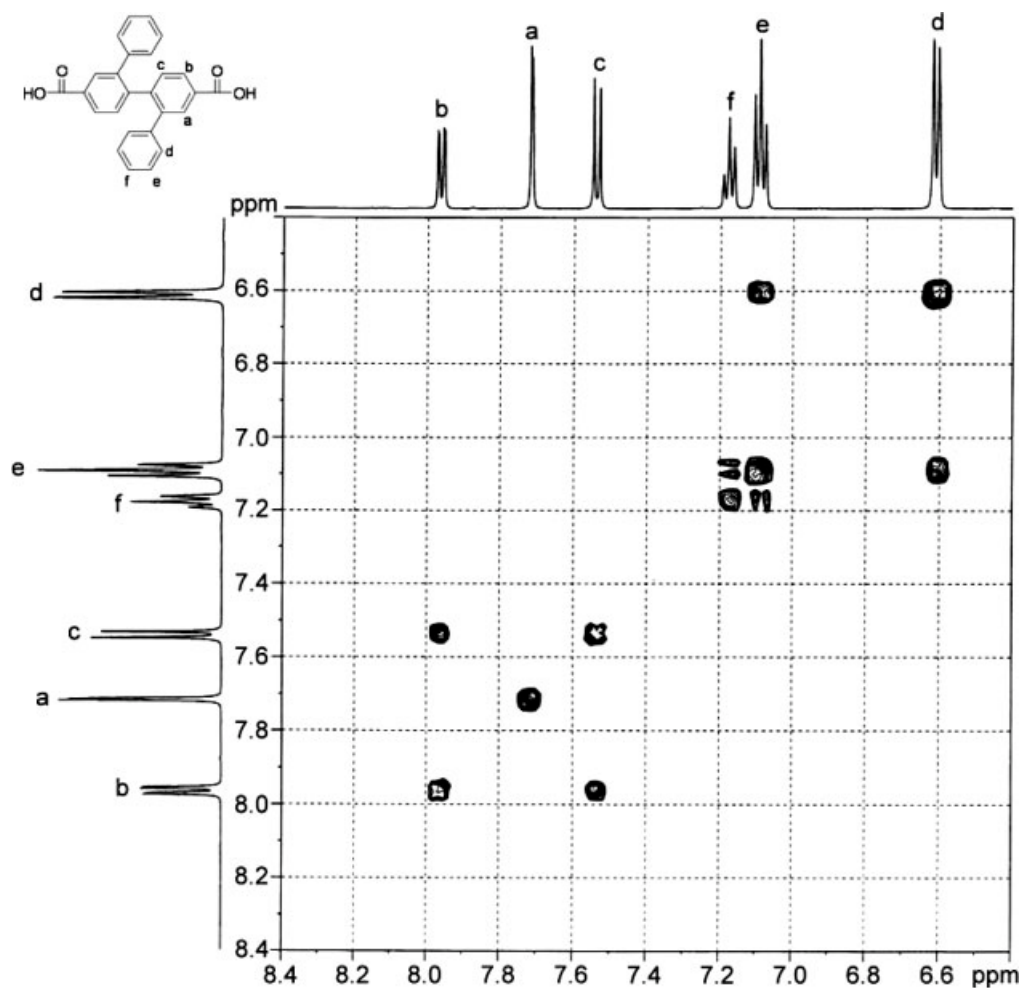


Figure 4. H-H COSY spectrum of diacid **4** in  $\text{DMSO-}d_6$ .



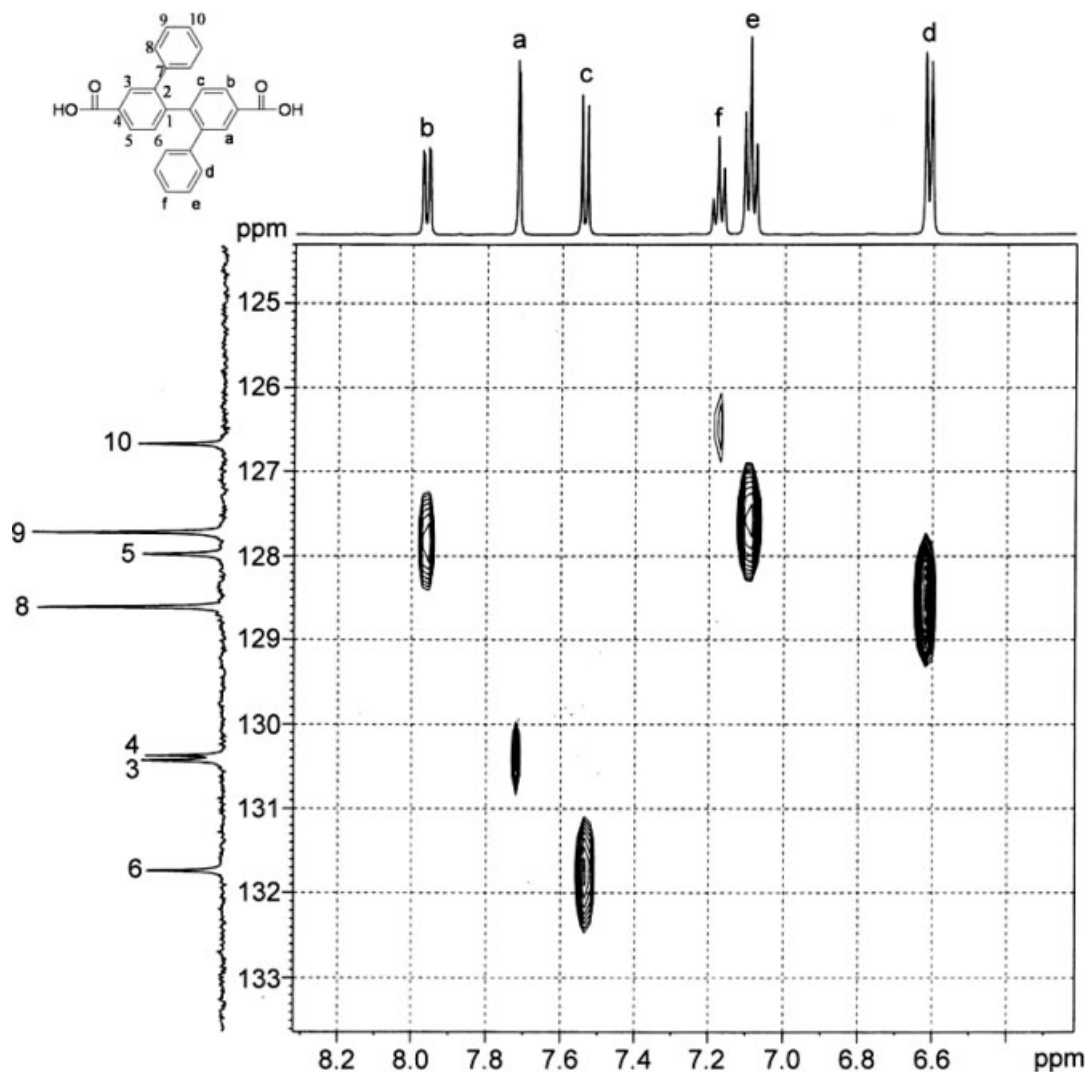


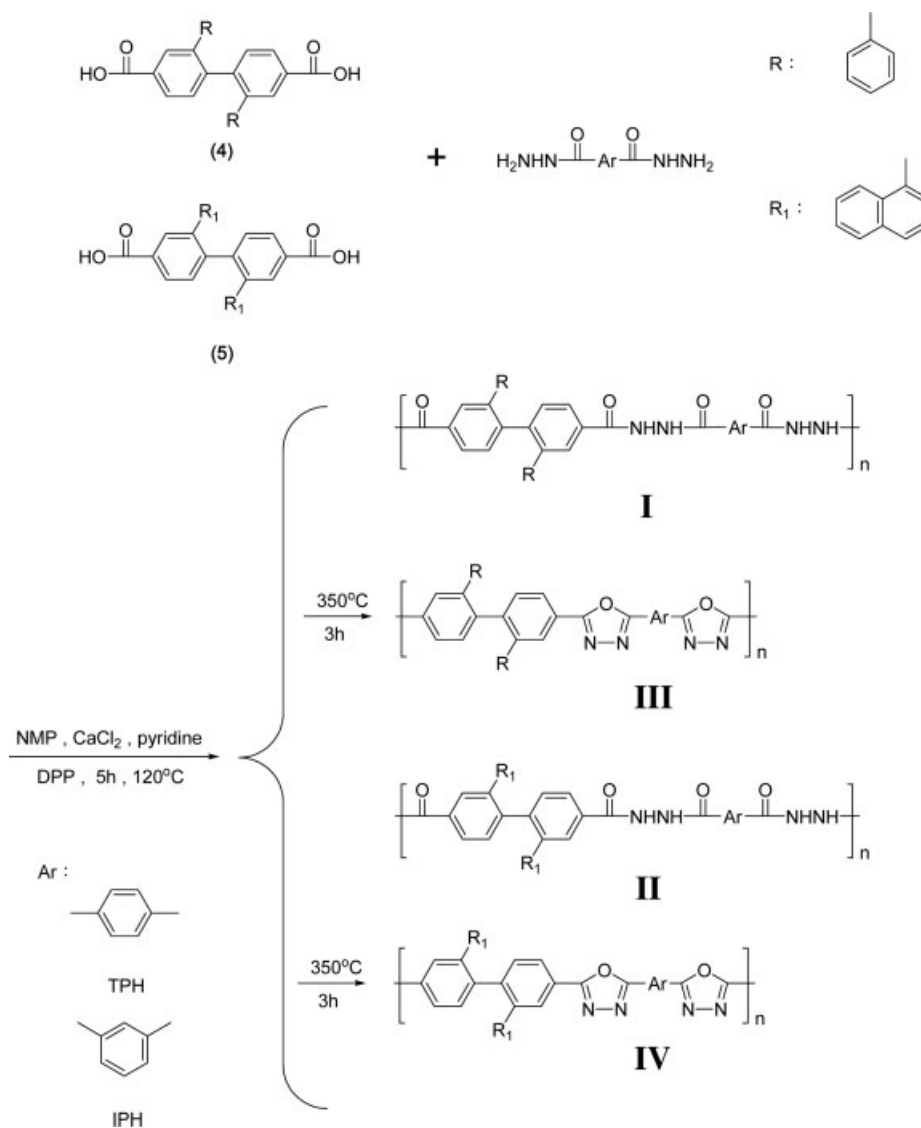
Figure 5. C-H HMQC spectrum of diacid **4** in DMSO- $d_6$ .

poly(1,3,4-oxadiazole) **IV-TPH**, as shown by the disappearance of the *N*-H stretching absorption at  $3247\text{ cm}^{-1}$  and the carbonyl peak at  $1664\text{ cm}^{-1}$ . One of the characteristic bands of 1,3,4-oxadiazole ring vibration were observed at  $1080\text{ cm}^{-1}$  (C—O—C str.). The absorption band due to oxadiazole C = N stretching was probably buried in the strong absorption bands  $1500\text{--}1600\text{ cm}^{-1}$  due to the skeletal vibration of benzene rings. DSC also could be used to investigate cyclization to the oxadiazole structure. A typical pair of DSC curves of polyhydrazide **II-TPH** and poly(1,3,4-oxadiazole) **IV-TPH** are illustrated in Figure 7. The main endothermic peak revealed the cyclodehydration reaction of the hydrazide group with water evolution in the range of  $300\text{--}400\text{ }^\circ\text{C}$ . The obtained poly(1,3,4-

oxadiazole)s had inherent viscosities in the range of  $0.26\text{--}0.50\text{ dL/g}$ .

#### Basic Properties of the Polymers

The X-ray diffraction studies of the polyhydrazides and poly(1,3,4-oxadiazole)s indicated that all the polymers were essentially amorphous. The solubility behavior of these polymers are summarized in Table 1. These polyhydrazides exhibited good solubility in various solvents such as NMP, DMAc, DMF, DMSO, and *m*-cresol. The thermally cured poly(1,3,4-oxadiazole)s showed a decreased solubility as compared with their hydrazide precursors, but at least could be dissolved in hot NMP. The amorphous nature and good solubility can be attributed to the



**Scheme 2.** Synthesis of polyhydrazides and poly(1,3,4-oxadiazole)s.

**Table I.** Solubility of Aromatic Polyhydridizes and Poly(1,3,4-oxadiazole)s

| Code    | $\eta_{\text{inh}}^{\text{a}}$ (dL/g) | Solvent |      |     |      |                  |     |                 |
|---------|---------------------------------------|---------|------|-----|------|------------------|-----|-----------------|
|         |                                       | NMP     | DMAc | DMF | DMSO | <i>m</i> -Cresol | THF | $\text{CHCl}_3$ |
| I-IPH   | 0.36                                  | ++      | ++   | ++  | ++   | ++               | –   | –               |
| I-TPH   | 0.71                                  | ++      | ++   | ++  | ++   | ++               | –   | –               |
| II-IPH  | 0.34                                  | ++      | ++   | ++  | ++   | ++               | –   | –               |
| II-TPH  | 0.97                                  | ++      | ++   | ++  | ++   | ++               | –   | –               |
| III-IPH | 0.45                                  | +h      | ±    | ±   | ±    | ±                | –   | –               |
| III-TPH | 0.42                                  | +h      | ±    | –   | ±    | ±                | –   | –               |
| IV-IPH  | 0.26                                  | +h      | ±    | ±   | ±    | ±                | –   | –               |
| IV-TPH  | 0.50                                  | +h      | ±    | –   | ±    | ±                | –   | –               |

++, soluble at room temperature; +h, soluble on heating; ±, partially soluble or swelling on heating; –, insoluble even on heating.

<sup>a</sup> Measured at a polymer concentration of 0.5 g/dL in NMP at 30 °C.

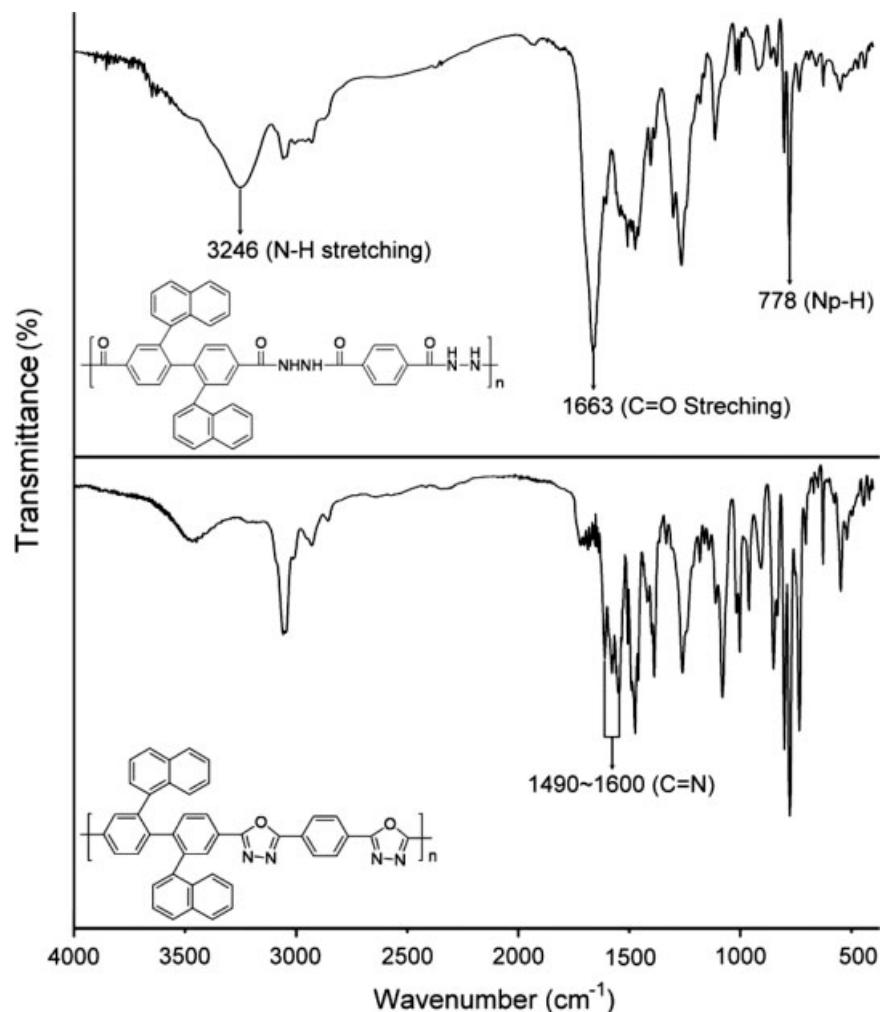


**Figure 6.** IR spectra of polyhydrazide **II-TPH** and poly(1,3,4-oxadiazole) **IV-TPH** films.

introduction of bulky phenyl or naphthyl units along the twisted noncoplanar rigid-rod polymer backbone. Thus, the good solubility makes these polymers as potential candidates for practical application by spin- or dip-coating processes.

DSC, TGA, and TMA were used to evaluate the thermal properties of all the polymers, and the results are summarized in Table 2. These hydrazide polymers showed a distinct  $T_g$  centered in the range 187–234 °C. As can be seen from the DSC thermograms, all the hydrazide polymers could be completely converted to the corresponding oxadiazole polymers when heated to 400 °C at a scan rate 20 °C/min in nitrogen. Because of the increasing rigidity of polymer main chain, all the oxadiazole polymers showed increased  $T_g$  values (252–283 °C) in comparison with the corresponding hydrazide polymers

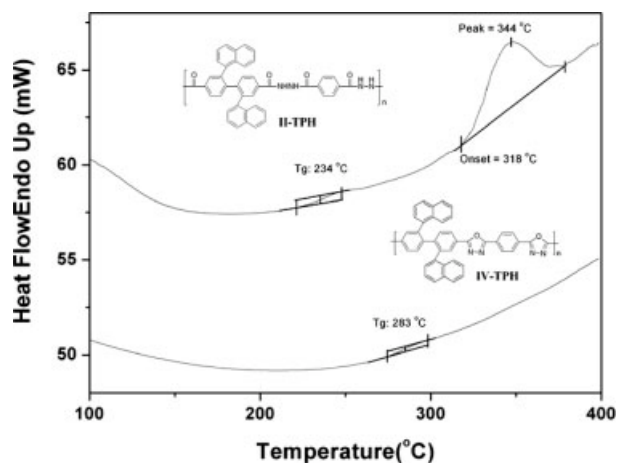


**Figure 7.** DSC traces of polyhydrazide **II-TPH** and poly(1,3,4-oxadiazole) **IV-TPH** with a heating rate of 20 °C/min in nitrogen.

**Table II.** Thermal properties of Polyhydrazides<sup>a</sup> and Poly(1,3,4-oxadiazole)s<sup>b</sup>

| Polyhydrazide |            |            |            | Poly(1,3,4-oxadiazole) |                         |                         |                           |     |                              |     |  |
|---------------|------------|------------|------------|------------------------|-------------------------|-------------------------|---------------------------|-----|------------------------------|-----|--|
| Code          | $T_g$ (°C) | $T_s$ (°C) | $T_p$ (°C) | Code                   | $T_g$ (°C) <sup>c</sup> | $T_s$ (°C) <sup>d</sup> | $T_d^5$ (°C) <sup>e</sup> |     | $T_d^{10}$ (°C) <sup>f</sup> |     | Char yield (wt %) <sup>g</sup><br>N <sub>2</sub> |
|               |            |            |            |                        |                         |                         | N <sub>2</sub>            | Air | N <sub>2</sub>               | Air |  |
| <b>I-IPH</b>  | 187        | 190        | 331        | <b>III-IPH</b>         | 252                     | 241                     | 440                       | 445 | 470                          | 470 | 55   |
| <b>I-TPH</b>  | 205        | 207        | 321        | <b>III-TPH</b>         | 272                     | 270                     | 450                       | 450 | 480                          | 480 | 58   |
| <b>II-IPH</b> | 190        | 185        | 328        | <b>IV-IPH</b>          | 270                     | 262                     | 485                       | 495 | 520                          | 530 | 65   |
| <b>II-TPH</b> | 234        | 232        | 344        | <b>IV-TPH</b>          | 283                     | 283                     | 495                       | 495 | 530                          | 535 | 63   |

<sup>a</sup> DSC data obtained from the DSC heating traces with a heating rate of 20 °C/min in nitrogen.  $T_g$ , the midpoint of baseline shift on the first DSC trace;  $T_s$ , softening temperature measured by TMA with a constant applied load of 10 mN at a heating rate of 10 °C/min;  $T_p$ , endothermic peak temperature.

<sup>b</sup> The polymer film samples were heated at 300 °C for 1 h prior to all the thermal analyses.

<sup>c</sup> The midpoint temperature of heat capacity jump on the DSC heating trace (from 50 to 400 °C at 20 °C/min) was defined as  $T_g$ .

<sup>d</sup> Softening temperature, taken as the onset temperature of the probe displacement on the TMA trace at a scan rate of 10 °C/min.

<sup>e</sup> Temperature at which 5 wt % loss occurred, recorded via TGA at a heating rate of 20 °C/min and a gas-flow rate of 20 cm<sup>3</sup>/min

<sup>f</sup> Temperature at which 10 wt % loss occurred.

<sup>g</sup> Residual weight percentage when heated 800 °C in nitrogen.

(187–234 °C). Typical TGA curves of a representative poly(1,3,4-oxadiazole) **IV-TPH** in both air and nitrogen atmospheres are shown in Figure 8; all the oxadiazole polymers exhibited good thermal stability without significant weight losses up to 400 °C in nitrogen. The 10% weight-loss temperatures ( $T_d^{10}$ ) of the poly(1,3,4-oxadiazole)s in nitrogen and air were recorded in the range of 470–530 and 470–535 °C, respectively. The amount of carbonized residue (char yield) of these polymers in nitrogen atmosphere was  $\gg 55\%$  at 800 °C. The high char yields of these polymers can be ascribed to their high aromatic content. The softening temperatures ( $T_s$ ) of the hydrazide polymer film samples were determined by the TMA method with a loaded penetration probe. They were obtained from the onset temperature of the probe displacement on the TMA trace. In most cases, the  $T_s$  values obtained by TMA are comparable with the  $T_g$  values measured by the DSC experiments (Table 2).

### Optical Properties

The optical properties of the polyhydrazides and poly(1,3,4-oxadiazole)s were investigated by UV–Vis and photoluminescence spectroscopy, and the results are summarized in Table 3. The optical absorption and photoluminescence spectra of monomers **4** and **5** in NMP solution are shown in Figure 9. The absorption bands of **4** exhibited peaks at 262 nm, which was contrib-

uted to the twisted structure between side chain phenyl and the main chain biphenyl groups. When these monomers were excited at the maximum absorption wavelength, the emission peaks of **4** and **5** were observed at 425 and 438 nm, respectively. These soluble polymers **I–IV** also exhibited maximum UV–Vis absorption bands at 261–320 nm in NMP solution, assignable to the  $\pi \rightarrow \pi^*$  transition resulting from the conjugation the aromatic rings. Their photoluminescence spectra in NMP solution and film showed maximum bands around 414–445 and 419–444 nm in the blue region for **I** and **II** series, respectively,

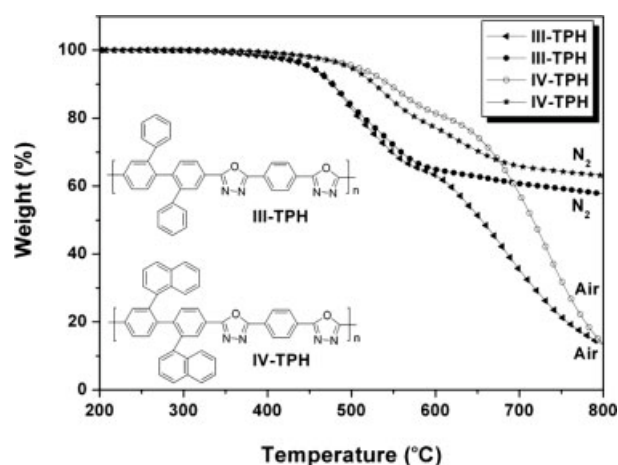


**Figure 8.** TGA thermograms of poly(1,3,4-oxadiazole)s **III-TPH** and **IV-TPH** at a scan rate of 20 °C/min.

**Table III.** Optical and Electrochemical Properties for Polyhydrazides and Poly(1,3,4-oxadiazole)s

| Index          | Solution $\lambda$ (nm) <sup>a</sup> |            |                           | Film $\lambda$ (nm)      |         |           | $E/N$ (vs. AgCl/Ag in DMF) |              |        | HOMO <sup>f</sup> (eV) |           | LUMO <sup>g</sup> (eV) |           |                    |
|----------------|--------------------------------------|------------|---------------------------|--------------------------|---------|-----------|----------------------------|--------------|--------|------------------------|-----------|------------------------|-----------|--------------------|
|                | Abs max                              | PL max     | $\Phi_F$ (%) <sup>b</sup> | $\lambda_0$ <sup>c</sup> | Abs max | Abs onset | PL max <sup>d</sup>        | First        | Second | $E_{\text{onset}}$     | $E_{1/2}$ | $E_{\text{onset}}$     | $E_{1/2}$ | $E_{\text{onset}}$ |
|                | $E_{1/2}$                            |            |                           |                          |         |           |                            |              |        |                        |           |                        |           |                    |
| <b>I-IPH</b>   | (262), 292                           | 420        | (0.9), 4.7                | 332                      | 305     | 348       | 419                        | <sup>h</sup> | -      | 3.56                   | -         | -                      | -         | -                  |
| <b>I-TPH</b>   | (263), 295                           | 414        | (0.5), 2.2                | 346                      | 305     | 353       | 422                        | -            | -      | 3.51                   | -         | -                      | -         | -                  |
| <b>II-IPH</b>  | 296                                  | 445        | 12.0                      | 333                      | 302     | 354       | 437                        | -            | -      | 3.50                   | -         | -                      | -         | -                  |
| <b>II-TPH</b>  | 286                                  | 440        | 3.8                       | 350                      | 305     | 357       | 444                        | -            | -      | 3.47                   | -         | -                      | -         | -                  |
| <b>III-IPH</b> | (267), 318                           | (419), 417 | (11.8), 38.0              | 349                      | 312     | 368       | 421                        | -1.79        | -      | -1.57                  | 3.37      | 5.90                   | 6.12      | 2.53               |
| <b>III-TPH</b> | (264), 342                           | (405), 404 | (8.3), 26.6               | 372                      | 338     | 386       | 417                        | -1.50        | -1.76  | -1.40                  | 3.21      | 6.03                   | 6.13      | 2.82               |
| <b>IV-IPH</b>  | 322                                  | 449        | 15.8                      | 348                      | 309     | 374       | 439                        | -1.76        | -      | -1.57                  | 3.31      | 5.87                   | 6.06      | 2.75               |
| <b>IV-TPH</b>  | 301                                  | 453        | 20.7                      | 370                      | 314     | 398       | 444                        | -1.46        | -1.75  | -1.37                  | 3.11      | 5.97                   | 6.06      | 2.86               |

<sup>a</sup> Spectra in NMP ( $10^{-5}$  mol/L).<sup>b</sup> The quantum yield in dilute solution was calculated in an integrating sphere with quinone sulfate as the standard ( $\Phi_F = 0.546$ ).<sup>c</sup> The cutoff wavelength from the UV-vis transmission spectra of polymer films.<sup>d</sup> They were excited at the  $\lambda_{\text{max}}$  wavelength for both solid and solution state.<sup>e</sup> The data were calculated by the equation:  $\text{gap} = 1240/\lambda_{\text{onset}}$  of polymer film.<sup>f</sup> HOMO = LUMO + gap.<sup>g</sup> The LUMO energy levels were calculated from cyclic voltammetry and were referenced to ferrocene (4.8 eV).<sup>h</sup> No discernible intensity could be observed.



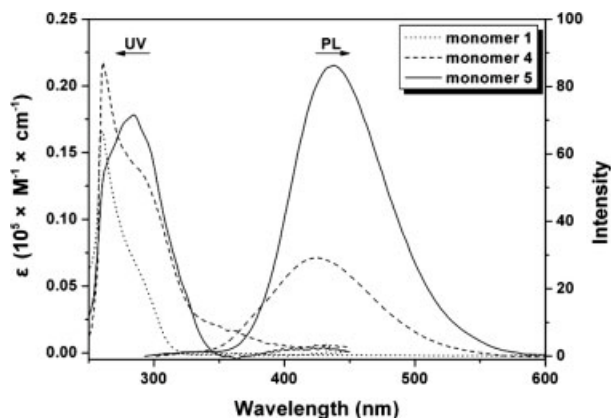


**Figure 9.** UV-Vis absorptions and PL spectra of diacid monomers **1**, **4**, and **5** in NMP solution ( $10^{-5}$  M).

(Figs. 10 and 11). These polymers exhibited similar spectra while the PL intensity of polyhydrazides **II** series is relatively greater than that of polyhydrazide **I** series. This phenomenon could be attributed to the naphthyl-substituted chromophore. Figures 10 and 11 showed the absorption bands of poly(1,3,4-oxadiazole) **III** and **IV** series with peaks at 318–342 and 301–322 nm, respectively, which could be attributed to  $\pi$ -conjugated 1,3,4-oxadiazole units. When the **III** and **IV** series were excited at the 1,3,4-oxadiazole units maximum absorption wavelength, the emission peaks of **III** and **IV** were observed at 404–419 and 449–453 nm, respectively. By comparing with **I-TPH**, the **III-TPH** emission peak

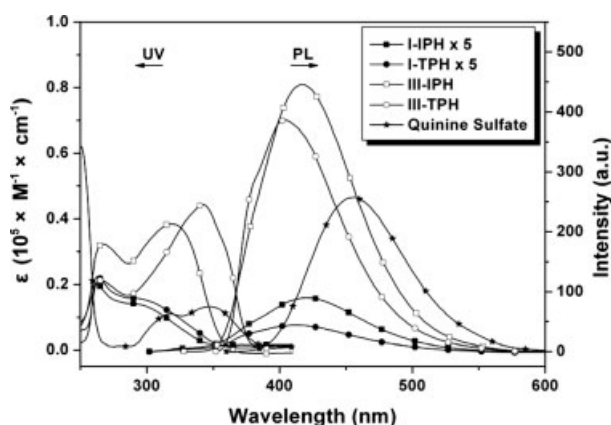


**Figure 10.** UV-Vis absorptions and PL spectra of polyhydrazides **I** and polyoxadiazoles **III** in NMP solution ( $10^{-5}$  M). Quinine sulfate dissolved in 1 N  $\text{H}_2\text{SO}_{4(\text{aq})}$  ( $10^{-5}$  M) was used as the standard ( $\Phi_F = 0.546$ ).

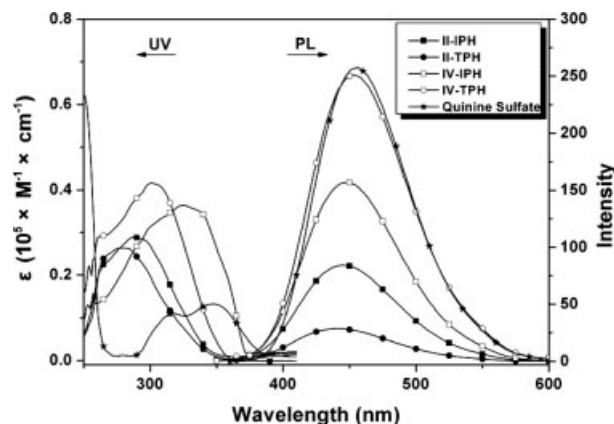


**Figure 11.** UV-Vis absorptions and PL spectra of polyhydrazides **II** and polyoxadiazoles **IV** in NMP solution ( $10^{-5}$  M). Quinine sulfate dissolved in 1N  $\text{H}_2\text{SO}_{4(\text{aq})}$  ( $10^{-5}$  M) was used as the standard ( $\Phi_F = 0.546$ ).

is blue-shifted from 414 to 404 nm, indicating that the efficient chromophore units shift from the side chain aromatics-substituted to main chain 1,3,4-oxadiazole moieties. The photoluminescence photographs of polyhydrazides and poly(1,3,4-oxadiazole)s in solution and film state under UV irradiation are shown in Figures 12 and 13. The cutoff wavelengths (absorption edge;  $\lambda_0$ ) from the UV-Vis transmittance spectra exhibited light-color and high optical transparency with cutoff wavelength in the range of 331–372 nm (Fig. 14).

### Electrochemical Properties

The electrochemical properties of the poly(1,3,4-oxadiazole)s were investigated by cyclic voltammetry, and the results are summarized in Table 3. The reduction behavior of poly(1,3,4-oxadiazole)s **III** and **IV** series was conducted by the cast films on an ITO-coated glass substrate as working electrode in dry *N,N*-dimethylformamide (DMF) containing 0.1 M of TBAP as electrolyte under nitrogen atmosphere. The poly(1,3,4-oxadiazole)s **III** and **IV** series undergo reversible reduction processes at  $E_{1/2} = -1.46$  to  $-1.79$  V ( $E_{\text{onset}} = -1.37$  to  $-1.57$  V). The poly(1,3,4-oxadiazole)s derived from **TPH** showed second reversible reduction peaks at  $E_{1/2} = -1.75$  to  $-1.76$  V, while the **IPH** series showed only one reversible reduction at  $-1.76$  to  $-1.79$  V. The typical cyclic voltammograms for poly(1,3,4-oxadiazole)s **III-TPH** and **IV-TPH** are shown in Figure 15. Comparing the electrochemical data, it was found

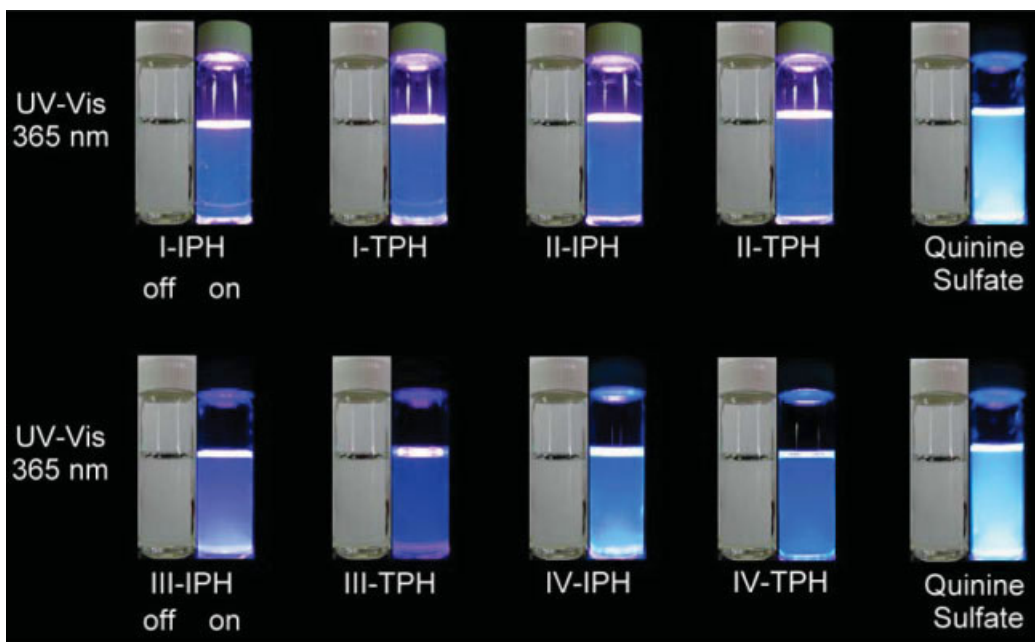


**Figure 12.** The photoluminescence of polyhydrazides and poly(1,3,4-oxadiazole)s solutions ( $10^{-5}$  M) by UV irradiation (excited at 365 nm). Quinine sulfate dissolved in 1 N  $\text{H}_2\text{SO}_{4(\text{aq})}$  ( $10^{-5}$  M) was used as the standard ( $\Phi_F = 0.546$ ).

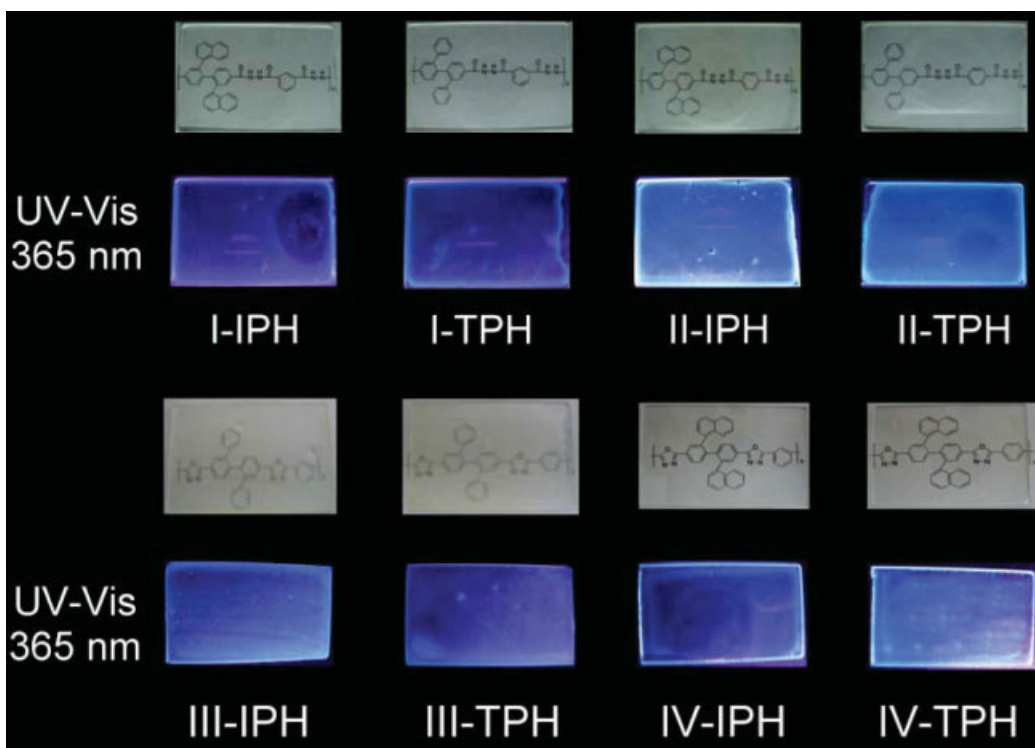


**Figure 13.** The photoluminescence of polyhydrazides and polyoxadiazole thin films I, II, III, and IV series (thickness: 6–15  $\mu\text{m}$ ) by UV irradiation (excited at 365 nm).

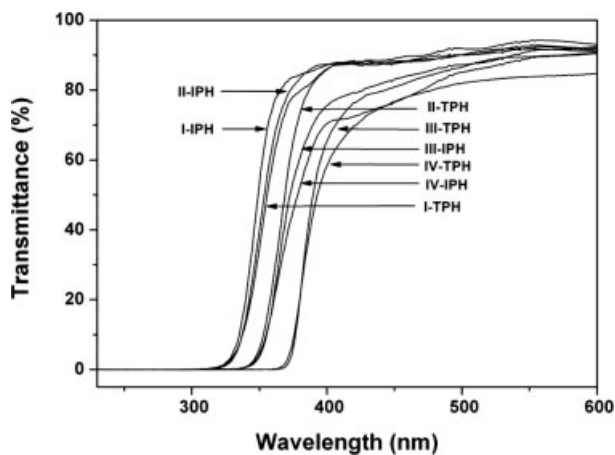


**Figure 14.** Transmission UV-Visible absorption spectra of polyhydrazides and poly(1,3,4-oxadiazole)s films (thickness: 6–15  $\mu\text{m}$ ).

that the reduction of poly(1,3,4-oxadiazole)s **IV-TPH** is much easier than **IV-IPH** due to the **TPH** system having more conjugation structure. The mechanism for the electrochemical reduction of poly(1,3,4-oxadiazole)s could be depicted as in Figure 16.<sup>36</sup> The energy levels of the HOMO and LUMO of the corresponding poly(1,3,4-oxadiazole)s can be determined from the reduction onset ( $E_{\text{onset}}$ ) and onset absorption wavelength of the UV-Vis irradiation, and the results are listed in Table 3. For example (Fig. 15), the reduction onset for poly(1,3,4-oxadiazole) **IV-TPH** has been determined as  $-1.37\text{ V versus Ag/AgCl}$ . The external ferrocene/ferrocenium ( $\text{Fc}/\text{Fc}^+$ ) redox standard  $E_{1/2}$  is  $0.48\text{ V versus Ag/AgCl}$  in DMF. Assuming that the HOMO energy for the  $\text{Fc}/\text{Fc}^+$  standard is  $4.80\text{ eV}$  with respect to the zero vacuum level, the LUMO energy for poly(1,3,4-oxadiazole) **IV-TPH** has been evaluated to be  $2.95\text{ eV}$ .

## CONCLUSIONS

The newly phenyl and naphthyl-substituted rigid-rod aromatic dicarboxylic acids, 2,2'-diphenylbiphenyl-4,4'-dicarboxylic acid (**4**) and 2,2'-di(1-naphthyl)biphenyl-4,4'-dicarboxylic acid (**5**) were successfully synthesized in high purity and good yield. Novel aromatic polyhydrazides were prepared from the dicarboxylic acids **4** and **5** with terephthalic dihydrazide and isophthalic dihydrazide, respectively, and were thermally cyclodehydrated into the corresponding poly(1,3,4-oxa-

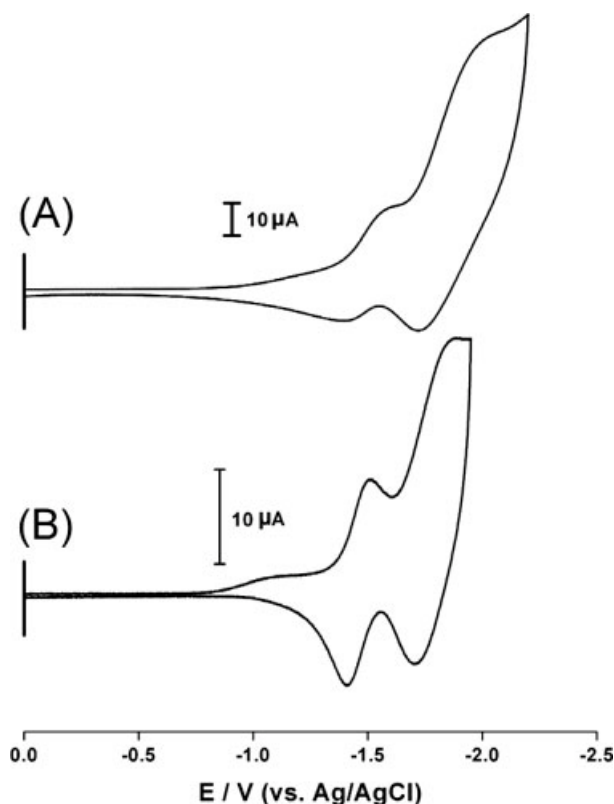


**Figure 15.** Cyclic voltammograms of poly(1,3,4-oxadiazole)s **III-TPH** and **IV-TPH** films onto an indium tin oxide (ITO)-coated glass substrate in DMF<sub>(aq)</sub> containing 0.1 M TBAP. Scan rate: 2.0 V/s. (A) reduction potential of poly(1,3,4-oxadiazole) **III-TPH** (B) reduction potential of poly(1,3,4-oxadiazole) **IV-TPH**.

diazole)s. The introduction of the bulky phenyl or naphthyl-substituted groups into the polymer side chain disrupts the coplanarity of aromatic units in chain packing, which increases the between-chains spaces or free volume thus enhancing solubility of the formed poly(1,3,4-oxadiazole)s. All the polymers were amorphous with high optical transparency from UV-Vis transmittance measurement with cutoff wavelength in the range of 332–372 nm. The polyhydrazides and poly(1,3,4-oxadiazole)s exhibited blue fluorescence emission maximum at 414–445 and 404–453 nm in NMP solution with quantum yields of 2.2–12.0 and 15.8–38.0%, respectively. All obtained poly(1,3,4-oxadiazole)s revealed stable reduction redox peaks at the applied potential in the range of  $-1.46$  to  $-1.79\text{ V}$ . Thus, our novel polyhydrazides and poly(1,3,4-oxadiazole)s have a great potential as a new blue-emitting electro-transporting materials due to their proper LUMO values, excellent

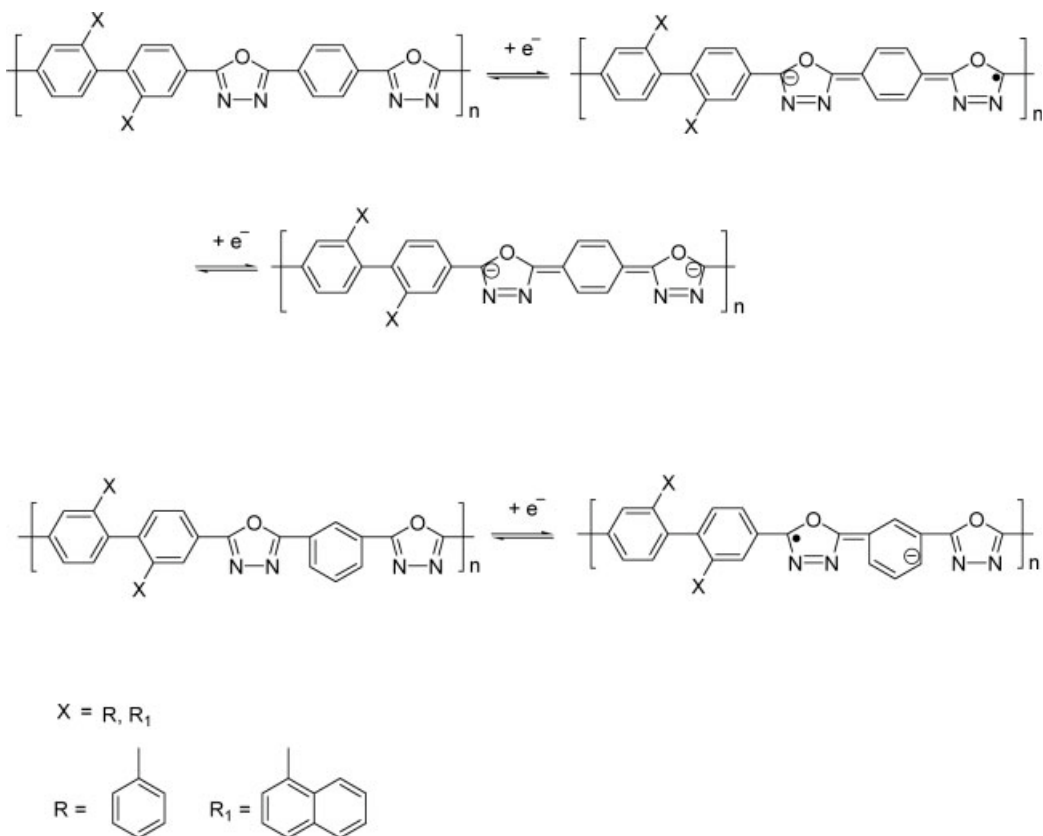


**Figure 16.** Reaction scheme of the electrochemical reduction of poly(1,3,4-oxadiazole)s in an aprotic medium.

thermal stability, and good fluorescence quantum efficiency.

We are grateful to the National Science Council of the Republic of China for financial support of this work.

## REFERENCES AND NOTES

- Cassidy, P. E. *Thermally Stable Polymers: Synthesis and Properties*; Marcel Dekker: New York, 1980; p 179.
- Nanjan, M. J. In *Encyclopedia of Polymer Science and Engineering*; Mark, J. F.; Bikales, N. M.; Overberger, C. G.; Menges, G.; Kroschwitz, J. I., Eds.; Wiley: New York, 1988; Vol. 12.
- Kraft, A.; Grimsdale, A. C.; Holmes, A. B. *Angew Chem Int Ed* 1998, 37, 402.
- Hsieh, B. Y.; Yeh, K. M.; Chen, Y. *J Polym Sci Part A: Polym Chem* 2005, 43, 5009.
- Liou, G. S.; Hsiao, S. H.; Su, T. H. *J Polym Sci Part A: Polym Chem* 2005, 43, 3245.
- Mikroyannidis, J. A.; Hlídková, H.; Výprachtický, D.; Cimrová V. *J Polym Sci Part A: Polym Chem* 2005, 43, 3079.
- Chen, S. H.; Chen, Y. *J Polym Sci Part A: Polym Chem* 2004, 42, 5900.
- Mikroyannidis, J. A.; Barberis, V. P.; Ding, L.; Karasz, F. E. *J Polym Sci Part A: Polym Chem* 2004, 42, 3212.
- Chen, S. H.; Chen, Y. *J Polym Sci Part A: Polym Chem* 2006, 44, 4514.
- Yu, W. L.; Meng, H.; Pei, J.; Huang, W.; Li, Y.; Heeger, A. J. *Macromolecules* 1999, 31, 4838.
- Huang, W.; Meng, H.; Yu, W. L.; Pei, J.; Chen, Z. K.; Lai, Y. H. *Macromolecules* 1999, 32, 118.
- Song, S. Y.; Jang, M. S.; Shim, M. K.; Hwang, D. H.; Zyung, T. *Macromolecules* 1999, 32, 1482.
- Hwang, S. W.; Chen, Y. *Macromolecules* 2002, 35, 5438.
- Hedrich, J. L. *Polymer* 1992, 33, 3375.
- Thaemlitz, C. J.; Weikeil, W. J.; Cassidy, P. E. *Polymer* 1992, 33, 3278.
- Hensema, E. R.; Sena, M. E. R.; Mulder, M. H. V.; Smolders, C. A. *J Polym Sci Part A: Polym Chem* 1994, 32, 527.
- Saegusa, Y.; Iwasaki, T.; Nakamura, S. *Macromol Chem Phys* 1997, 198, 1799.
- Maglio, G.; Palumbo, R.; Tortora, M.; Trifuoggi, M.; Varricchio, G. *Polymer* 1998, 39, 6407.
- Hsiao, S. H.; Yu, C. H. *J Polym Sci Part A: Polym Chem* 1998, 36, 1847.

20. Hsiao, S. H.; Dai, L. R.; He, M. S. *J Polym Sci Part A: Polym Chem* 1999, 37, 1169.
21. Peng, Z.; Bao, Z.; Galvin, M. E. *Adv Mater* 1998, 10, 680.
22. Chen, Z. K.; Meng, H.; Lai, Y. H.; Huang, W. *Macromolecules* 1999, 32, 4351.
23. Song, S. Y.; Jang, M. S.; Shim, H. K.; Song, I. S.; Kim, W. H. *Synth Met* 1999, 102, 1116.
24. Liaw, D. J.; Chang, F. C.; Leung, M.; Chou, M. Y.; Muellen, K. *Macromolecules* 2005, 38, 4024.
25. Kim, H. S.; Kim, Y. H.; Ahn, S. K.; Kwon, S. K. *Macromolecules* 2003, 36, 2327.
26. Kim, K. H.; Jang, S.; Harris, F. W. *Macromolecules* 2001, 34, 8925.
27. Lin, S. H.; Li, F.; Cheng, S. Z. D.; Harris, F. W. *Macromolecules* 1998, 31, 2080.
28. Chuang, K. C.; Kinder, J. D.; Hull, D. L.; McConville, D. B.; Youngs, W. J. *Macromolecules* 1997, 30, 7183.
29. Frazer, A. H.; Sweeny, W.; Wallenberger, F. T. *J Polym Sci Part A: Polym Chem* 1964, 2, 1157.
30. Hensema, E. R.; Boom, J. P.; Mulder, M. H. V.; Smolders, C. A. *J Polym Sci Part A: Polym Chem* 1994, 32, 513.
31. Janietz, S.; Analauf, S. *Macromol Chem Phys* 2002, 203, 427.
32. Yang, C. F.; Chen, H. D.; Yang, K. H.; Leung, M. K.; Wu, C. C.; Yang, C. C.; Wang, C. C.; Fann, W. S. *Mater Sci Eng B* 2001, 85, 236.
33. Leung, M. K.; Chou, M. Y.; Su, Y. O.; Chiang, C. L.; Chen, H. L.; Yang, C. F.; Yang, C. C.; Lin, C. C.; Chen, H. T. *Org Lett* 2003, 5, 839.
34. Higashi, F.; Ishikawa, M. *J Polym Sci Polym Chem Ed* 1980, 18, 2905.
35. Demas, J. N.; Crosby, G. A. *J Phys Chem* 1971, 75, 991.
36. Kress, L.; Neudeck, A.; Petr, A.; Dunsch, L. *J Electroanal Chem* 1996, 414, 31.